Autosomal-Dominant Distal Myopathy Associated with a Recurrent Missense Mutation in the Gene Encoding the Nuclear Matrix Protein, Matrin 3

Jan Senderek,[1,2,*] Sean M. Garvey,[3,4] Michael Krieger,[2] Velina Guergueltcheva,[5] Andoni Urtizberea,[6] Andreas Roos,[2] Miriam Elbracht,[2] Claudia Stendel,[1,2] Ivailo Tournev,[5] Violeta Mihailova,[5] Howard Feit,[7] Jeff Tramonte,[8] Peter Hedera,[9] Kristy Crooks,[4] Carsten Bergmann,[2] Sabine Rudnik-Schöneborn,[2] Klaus Zerres,[2] Hanns Lochmüller,[10] Eric Seboun,[11] Joachim Weis,[12] Jacques S. Beckmann,[13] Michael A. Hauser,[4] and Charles E. Jackson[14]

Distal myopathies represent a heterogeneous group of inherited skeletal muscle disorders. One type of adult-onset, progressive autosomal-dominant distal myopathy, frequently associated with dysphagia and dysphonia (vocal cord and pharyngeal weakness with distal myopathy [VCPDM]), has been mapped to chromosome 5q31 in a North American pedigree. Here, we report the identification of a second large VCPDM family of Bulgarian descent and fine mapping of the critical interval. Sequencing of positional candidate genes revealed precisely the same nonconservative S85C missense mutation affecting an interspecies conserved residue in the *MATR3* gene in both families. *MATR3* is expressed in skeletal muscle and encodes matrin 3, a component of the nuclear matrix, which is a proteinaceous network that extends throughout the nucleus. Different disease related haplotype signatures in the two families provided evidence that two independent mutational events at the same position in *MATR3* cause VCPDM. Our data establish proof of principle that the nuclear matrix is crucial for normal skeletal muscle structure and function and put VCPDM on the growing list of monogenic disorders associated with the nuclear proteome.

The distal myopathies are a clinically and pathologically heterogeneous group of genetic disorders in which the distal muscles of the upper and the lower limbs are selectively or disproportionately affected.[1,2] Comparison of the different forms of distal myopathy has shown considerable phenotypic variability, both in terms of the age at onset and the pattern of muscle involvement. Some subtypes of distal myopathy clinically or genetically overlap with the inclusion body myopathies (summarized in MIM 605637 for IBM3) and the limb-girdle muscular dystrophies (summarized in MIM 159000 for LGMD1A and MIM 253600 for LGMD2A). Distal myopathies are caused by mutations in genes encoding proteins associated with the plasma membrane (dysferlin [MIM 603009][3,4] and caveolin-3 [MIM 601047][5]), with the sarcomere (titin [MIM 188840][6] and myosin [MIM 160760][7]), and with posttranslational protein modifications (UDP-N-acetylglucosamine-2-epimerase [MIM 603824]).[8]

A decade ago, we described in this journal an adult-onset autosomal-dominant distal myopathy often complicated by vocal cord paralysis (vocal cord and pharyngeal weakness with distal myopathy, VCPDM [MIM 606070]).[9] Genome-wide linkage analysis in a single large North American pedigree revealed that the VCPDM locus mapped to a 12 cM (11.8 Mb) interval on chromosome 5q between microsatellite markers D5S1995 and D5S436. First symptoms developed at the age of 35–57 years and the most frequent initial manifestation was ankle dorsiflexion weakness and foot drop. The disease had a slowly progressive course with involvement of the feet and hands and eventually an effect on shoulder and pelvic muscles. Vocal cord or swallowing dysfunction occurred in most cases. Electromyogram (EMG) and nerve conduction studies indicated a myopathy, and the levels of serum creatine phosphokinase (CPK) were usually only mildly or moderately elevated (at maximum 8× the upper limits of normal). Analysis of muscle biopsies showed myopathic changes including variations in fiber size, fiber splitting, and subsarcolemmal rimmed vacuoles.

We were now able to expand the family because another two siblings were now definitely afflicted with the disease. These individuals belong to an additional branch of the family and had not been included in the 1998 paper (for a comparison of clinical data, see Table 1). Analysis of microsatellite markers and haplotype reconstruction disclosed a critical recombination event between D5S2009 and D5S21116 in both patients. On the basis of the available genomic sequence of chromosome 5q31, a set of

[1]Institute of Cell Biology, ETH Zürich, 8093 Zürich, Switzerland; [2]Institute of Human Genetics, Aachen University of Technology, 52074 Aachen, Germany; [3]Robert M. Berne Cardiovascular Research Center, Division of Cardiovascular Medicine, University of Virginia, Charlottesville, VA 22908, USA; [4]Center for Human Genetics, Duke University Medical Center, Durham, NC 27710, USA; [5]Clinic of Neurology, Alexandrovska University Hospital, Sofia Medical University, 1431 Sofia, Bulgaria; [6]Hôpital Marin de Hendaye, 64701 Hendaye, France; [7]Department of Neurology, Henry Ford Hospital, Detroit, MI 48202, USA; [8]Department of Neurology, Scott and White Memorial Hospital, Temple, TX 76508, USA; [9]Department of Neurology, Vanderbilt University, Nashville, TN 37240, USA; [10]Institute of Human Genetics, Newcastle upon Tyne, NE1 3BZ, UK; [11]Division de Génétique et de Microbiologie, Université Pierre et Marie Curie, 75005 Paris, France; [12]Institute of Neuropathology, Aachen University of Technology, 52074 Aachen, Germany; [13]Department and Service of Medical Genetics, University of Lausanne and Centre Hospitalier Universitaire Vaudois, 1005 Lausanne, Switzerland; [14]Department of Medicine, Scott & White Memorial Hospital, Temple, TX 76508, USA
*Correspondence: jan.senderek@cell.biol.ethz.ch
DOI 10.1016/j.ajhg.2009.03.006.

Table 1. Comparison of Clinical Features

Family	Patient	Age at Onset (years)	First Symptom	Distal weakness		Shoulder Weakness	Swallowing/ Vocal Cord Dysfunction	CPK
				Legs	Hands			
NA[a]		Mean: 45 (Range: 35–57)	Legs: 7/11 Hands: 2/11 Pharyngeal: 2/11	12/12	10/12	4/12	9/12	Normal, 8×
NA	DM73.3	48	Legs	+	+	−	−	2×
NA	DM73.4	45	Legs	+	+	−	+	2×
BG	IV.9	43	Legs	+	+	−	−	ND
BG	V.6	47	Legs	+	+	+	+	ND
BG	V.9	40	Legs	+	+	+	+	2×
BG	V.11	54	Legs	+	+	−	ND	ND
BG	V.13	52	Legs	+	+	−	ND	ND
BG	V.15	42	Legs	+	−	−	ND	ND
BG	V.17	46	Hands	−	+	−	ND	ND
BG	V.23	49	Legs	+	+	+	−	4×
BG	V.27	40	Legs	+	+	+	+	3×
BG	V.30	36	ND	+	−	−	ND	2×

NA, North American family; BG, Bulgarian family; ND, not determined; CPK, creatine phosphokinase;
[a] Data summarized from Feit et al.[9]

additional densely spaced short tandem repeat (STR) polymorphisms was deduced. Using these markers, we mapped the recombination event between AC008667A and AC008667C, thereby reducing the candidate interval from 11.8 Mb to 5.9 Mb. By using newly established STRs, we could also narrow down the site of the recombination at the centromeric border of the VCPDM region. The refined critical region spanned 5.37 Mb between STR markers sara2AC and AC008667C (Figure 1, for details referring to newly established STR markers, see Table S1 available online). We then checked a series of ten families with autosomal-dominant distal myopathy with clinical features resembling VCPDM for compatibility with linkage to the VCPDM region on chromosome 5q31. We identified a multigenerational Bulgarian family (Figure 2) with a typical VCPDM phenotype (for a comparison of clinical data, see Table 1). With a set of 12 available DNA samples from this family, genotyping and haplotype reconstruction of STR markers D5S458, D5S500, D5S594, and D5S2116 established linkage to the VCPDM interval. A maximum two-point LOD score (Zmax) of 3.35 was obtained at recombination fraction (θ) 0 for marker D5S500, but no new recombination events, allowing a further restriction of the VCPDM interval, were identified. VCPDM-disease-associated haplotypes differed between the North American and Bulgarian samples. The review board for medical ethics at Aachen University of Technology gave approval for sample collection and molecular genetic studies in conjunction with local approval in the United States and Bulgaria.

The May 2004 version of the human genome assembly displayed 56 genes represented in the NCBI Reference Sequence (RefSeq) collection between the newly established borders of the VCPDM critical region. The most apparent candidate gene within this interval was *myotilin* (*MYOT* [MIM 604103]). Myotilin contributes to sarcomere assembly and promotes actin crosslinking and sarcomeric integrity,[10] and *MYOT* mutations have been shown to cause Limb-Girdle Muscular Dystrophy Type 1A (LGMD1A),[11] a small fraction of myofibrillar myopathy cases (MFM [MIM 609200]),[12] and spheroid body myopathy [MIM 182920].[13] However, we found no *MYOT* abnormalities on the genomic, transcript, and protein level in the North American VCPDM family.[14] Moreover, no *MYOT* mutation was detected in the Bulgarian pedigree

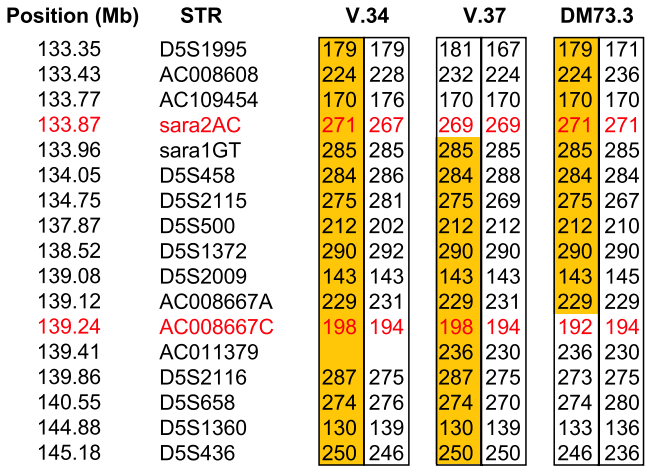

Figure 1. Refinement of the VCPDM Interval in the North American VCPDM Family
A subset of markers used in this study is given in centromeric to telomeric orientation. The physical map positions are according to the UCSC March 2006 freeze. Patient V.34 carries the full-blown disease haplotype. Recombination events in patient V.37 and patient DM73.3 (newly identified patient from the North American family) excluded markers sara2AC and AC008667C (printed in red), respectively, delimiting a 5.37 Mb region.

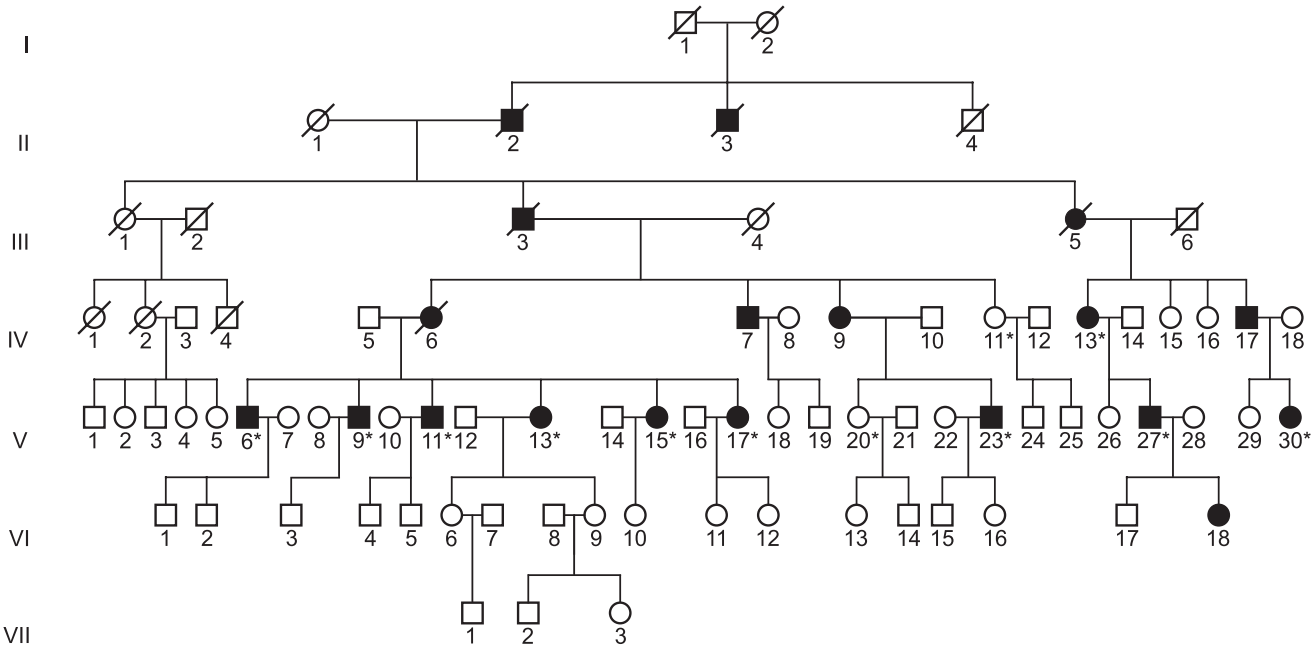

Figure 2. Pedigree of the Bulgarian VCPDM Family
Individuals of whom DNA samples were available are marked by asterisks.

by sequencing of all coding exons. These results provided strong evidence that myotilinopathies and VCPDM are not allelic disorders. Therefore, we prioritized the remaining annotated sequences with respect to skeletal muscle biology and disease. We used information from publicly available databases and characterized proteins in silico by BLAST alignments to protein database entries and by comparison of domain composition and organization with the SMART algorithm. We also investigated positional candidate genes for structural and functional homology with the known proteins involved in distal myopathies and related disorders. The entire coding and adjacent intronic regions of 20 candidate genes for a distal myopathy were analyzed by direct sequencing (Table 2).

We detected the same c.254C→G change in both families in exon 2 of the *MATR3* gene (MIM 164015) (Figure 3A, for primer sets used to analyze the *MATR3* gene, see Table S2), whereas no pathogenic mutations

Table 2. Positional Candidate Genes Analyzed

Gene Name	Expression in Skeletal Muscle	Entrez Gene Identifier	OMIM Number	Strand	Genomic Position		Number of Coding Exons
					Start	End	
SEC24A	+	10802	607183	+	134012378	134091500	23
C5orf14	+	79770	–	+	134237359	134265222	5
DCOHM	+	84105	609836	+	134268709	134326235	4
LOC153328	unknown	153328	–	+	135198264	135236335	6
FBXL21	+	26223	609087	+	135300162	135305266	4
SPOCK	+	6695	602264	–	136338886	136862917	10
KLHL3	+	26249	605775	–	136981088	137099678	15
C5orf5	+	51306	609371	–	137301541	137396701	21
BRD8	+	10902	602848	–	137520472	137542257	29
C5orf6	+	51307	609372	+	137701603	137713315	4
C5orf7	+	51380	609373	+	137716184	137800615	24
HSPA9B	+	3313	600548	–	137918923	137939014	17
SIL1	+	64374	608005	–	138310309	138561964	9
MATR3	+	9782	164015	+	138657254	138694029	14
PAIP2	+	51247	605604	+	138705418	138733308	3
PACAP	+	51237	609447	–	138751156	138753504	4
DNAJC18	+	202052	–	–	138775279	138803038	8
TMEM173	+	340061	612374	–	138835733	138842476	6
UBE2D2	+	7322	602962	+	138920935	138988202	7
PSD2	+	84249	–	+	139155590	139204232	14

A

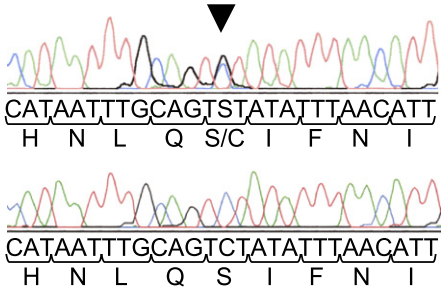

B

Position (Mb)	STR/SNP	NA	BG
137.88	D5S500	212	206
138.52	**D5S1372**	**290**	**300**
138.63	AC011404	169	169
138.67	*MATR3*, c.254C>G	G	G
138.68	**rs13178336**	**T**	**C**
138.68	rs12186596	A	A
138.68	**AC011404B**	**263**	**269**
138.69	rs10515507	G	G
138.81	**D5S594**	**433**	**441**
139.12	AC008667A	229	231

C

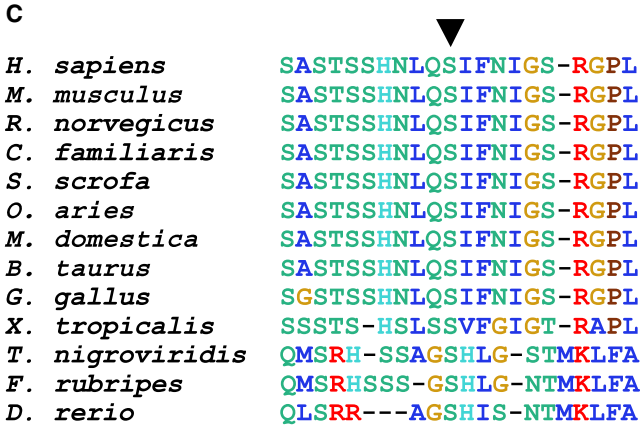

Figure 3. Identification of the VCPDM Mutation

(A) DNA sequence traces illustrating the c.254C→G, S85C mutation in the *MATR3* gene (upper panel) and the corresponding wild-type sequence (lower panel). The position of the single nucleotide exchange is marked with an arrowhead.

(B) Comparison of disease-associated haplotypes. The disease-associated haplotype in the North American family is shown under the column heading "NA"; the disease-associated haplotype in the Bulgarian pedigree is shown under the heading "BG." The phases of alleles have been determined for all markers. Intragenic markers and the mutation in exon 2 of the *MATR3* gene are boxed. The closest flanking and intragenic markers that show different alleles for the North American and Bulgarian samples are printed in red.

(C) Multiple sequence alignment of human matrin 3 and related sequences. The mutant serine 85 residue is marked by an arrowhead.

were identified in any of the other candidate genes. This mutation leads to an amino acid substitution from serine to cysteine at position 85 (S85C). We confirmed segregation of this change in both families. This mutation has not been deposited in the most recent release (build 129) of dbSNP, and 572 healthy controls (300 German, 164 white Northern American, and 108 Bulgarian) were negative for this nucleotide substitution. Analysis of haplotypes for closely flanking and intragenic SNP and STR markers showed no evidence of haplotype sharing between the North American and the Bulgarian VCPDM families (Figure 3B, for details referring to SNP and STR markers used, see Table S1). This indicates that these two kindreds with VCPDM are not closely related and suggests that the same *MATR3* mutation arose independently in each of them.

Matrin 3 is a 130 kDA (847 amino acid) nuclear protein with nuclear import and export motifs and several binding sites for DNA and RNA[15,16] (Figure S1A). Matrin 3 is highly conserved through evolution (96% sequence homology between human and rat orthologs) and expression is observed in a variety of tissues including skeletal muscle and lymphoblasts (HUGE protein database and Figures S1B and S1C). Matrin 3 is a component of the nuclear matrix, an insoluble network that is dispersed throughout the nucleus and that is operationally defined as being resistant to high salt or detergents.[17] Although the nature of the nuclear matrix is still under debate,[18] it has achieved prominence given that its components are associated with the protein machinery for transcription, RNA splicing, and DNA replication.[19] Moreover, accumulating experimental evidence suggests that the positioning of individual chromosomes in the interphase nucleus[20] is achieved by attachment of chromatin loops to the nuclear matrix at the so-called matrix attachment regions (MARs).[21,22] Although experimental evidence for a causal relationship is still lacking, the 3D organization of the genome in the interphase nucleus is believed to be an important factor for the orchestration of gene expression in the mammalian genome.[23]

The nuclear matrix is structurally and functionally connected with the nuclear lamina, the nuclear proteome associated with the inner leaflet of the nuclear envelope.[24–26] The role of the nuclear lamina in human diseases has been established during the last 15 years,[27] and the growing list of diseases of the nuclear envelope also includes neuromuscular conditions such as Emery Dreyfuss muscular dystrophy (MIM 310300; MIM 181350),[28,29] limb-girdle muscular dystrophy type 1B (MIM 159001),[30] and Charcot-Marie-Tooth neuropathy type 2B1 (MIM 605588).[31] Additional evidence for a role of the nuclear matrix in the pathophysiology of the skeletal muscle comes from very recent work on facio-scapulo-humeral dystrophy (FSHD [MIM 158900]) and X-linked myopathies. First, the partial deletion of the D4Z4 repeat array that causes FSHD[32] results in delocation of an adjacent MAR from the nuclear matrix. This alteration is expected to change chromatin structure and to release transcriptional repression of neighboring genes implicated in the genesis of FSHD.[33] Second, mutations in the *FHL1* gene (MIM 300163), encoding four-and-a-half LIM domain 1, cause clinically variable types of

X-linked myopathies (MIM 300695).[34–36] FHL2, a homolog of FHL1, has been reported to bind to the nuclear matrix protein NP220 and the splicing factor PSF, a known matrin 3 interaction partner.[37,38]

Currently, the effect of the identified S85C alteration on matrin 3 structure and function is not clear. Alterations of amino acid residues involved in nucleic acid binding may seriously impair the matrin 3 function. But the residues in contact with RNA and DNA are not close to the position shown here as changed (Figure S1A). However, assessment of the biochemical severity of the S85C change and the location and context of the altered amino acid in the protein sequence suggests that the mutation has functional consequences. With the Grantham scale,[39] which categorizes codon replacements into classes of chemical dissimilarity between the encoded amino acids, the c.254C→G missense mutation in matrin 3 was designated to be moderately radical according to the classification proposed by Li et al.[40] Given that disease-causing mutations are likely to occur at regions encoding conserved amino acid residues across species,[41] we studied cross-species conservation of regions surrounding the S85C alteration by using the ClustalW algorithm. We found that the residue S85 is conserved across a wide range of species including mammals, chicken, frog, and fish (Figure 3C). Further, we applied three in silico algorithms—the SIFT algorithm,[42] the PolyPhen algorithm,[43] and the subPSEC algorithm[44,45]—to predict the putative effect of the mutation on the protein. With SIFT, the S85C substitution was classified as intolerant according to the classification by Ng and Henikoff.[42] PolyPhen designated the S85C alteration as possibly damaging according to the classification by Xi et al.[46] Finally, the subPSEC program predicted the S85C change to cause a deleterious effect on protein function with the criteria proposed by Brunham et al.[47]

We had the opportunity to study a muscle biopsy of a Bulgarian VCPDM case. Morphological analysis of the frozen muscle biopsy specimen revealed end-stage myopathy. The muscle was largely replaced by proliferated fat and connective tissue (Figure 4A). We observed strikingly variable degrees of immunoreactivity of myonuclei for matrin 3 (Figures 4B and 4C), whereas all nuclei of a normal control muscle were strongly labeled after incubation with the matrin 3 antibody (Figure 4D). Autophagic vacuoles were encountered in several muscle fibers and myonuclei displayed various stages of nuclear degeneration (Figures 4E–4G). On the other hand, nuclei of cultured lymphoblasts obtained from a VCPDM patient did not disclose overt pathology (Figure S2A). However, fractionation of nuclear proteins showed that matrin 3 is almost exclusively confined to the insoluble fraction in VCPDM lymphoblasts, whereas in control lymphoblasts, a considerable proportion of matrin 3 occurs in the nucleic-acid binding protein fraction (Figure S2B). A similar shift of the subnuclear distribution was seen for the Myc-tagged S85C matrin 3 mutant compared to Myc-tagged wild-type matrin 3 upon overexpression in Cos7 cells. Immunofluorescence analysis of transfected matrin 3 in Cos7 cells ascertained that this observation did not arise from the formation of insoluble nuclear aggregates (Figures S2C and S2D). Although the present data suggest that muscle pathology in VCPDM might be related to changes of the matrin 3 expression level and/or intranuclear mobility functional studies are obviously needed to clarify how mutant matrin 3 affects skeletal muscle physiology.

A variety of mechanisms leading to myofiber degeneration could be involved in VCPDM pathogenesis: (1) modification of gene expression relative to abnormal chromatin organization: matrin 3 has been shown to regulate transcription rates through association with matrix attachment sites in vitro.[48] (2) Deregulation of nuclear mRNA export: together with p54nrb and PSF, matrin 3 controls the retention of hyperedited mRNAs in the nucleus to prevent their translation at the ribosome.[49] (3) Abnormal pre-mRNA splicing: matrin 3 was found to be coimmunoprecipitated with hLodestar/HuF2, together with CDC5L, hnRNP A1, hnRNP A2/B1, and chromokinesin, suggesting it is also involved in pre-mRNA splicing.[50,51] (4) Alterations of the nuclear proteome: matrin 3 also plays a role in the nuclear import of proteins,[52] thereby potentially altering nuclear functions. As a matter of course, these putative disease mechanisms are not necessarily mutually exclusive.

To our knowledge, this study is the first report of the association of a mutation in a gene encoding a nuclear matrix protein with a human hereditary disease. Our observations of the same *MATR3* gene mutation in two unrelated kindreds with VCPDM that results in a nonconservative substitution of an interspecies conserved amino acid and that was absent in control subjects strongly support the pathogenic significance of this mutation. Our discovery of *MATR3* mutations as the cause of VCPDM will aid genetic testing and counselling of patients with distal myopathies. Moreover, the knowledge about the involvement of the nuclear matrix protein matrin 3 in an inherited myopathy provides a path to a better understanding of the development, degeneration, and regeneration of skeletal muscle. Identification of the underlying mechanisms of muscle fiber damage in inherited myopathies may hold promise for the development of therapeutic interventions in these (usually rare) entities and, perhaps, in the (usually more frequent) sporadic forms of skeletal muscle disorders. In this way, our data are relevant for patient and family care, for basic science, and—hopefully—future options to treat neuromuscular disorders.

Supplemental Data

Supplemental Data include two figures and two tables and can be found with this article online at http://www.ajhg.org/.

Acknowledgments

We are indebted to the members of the families with distal myopathies for their participation in this study. J. Senderek is a

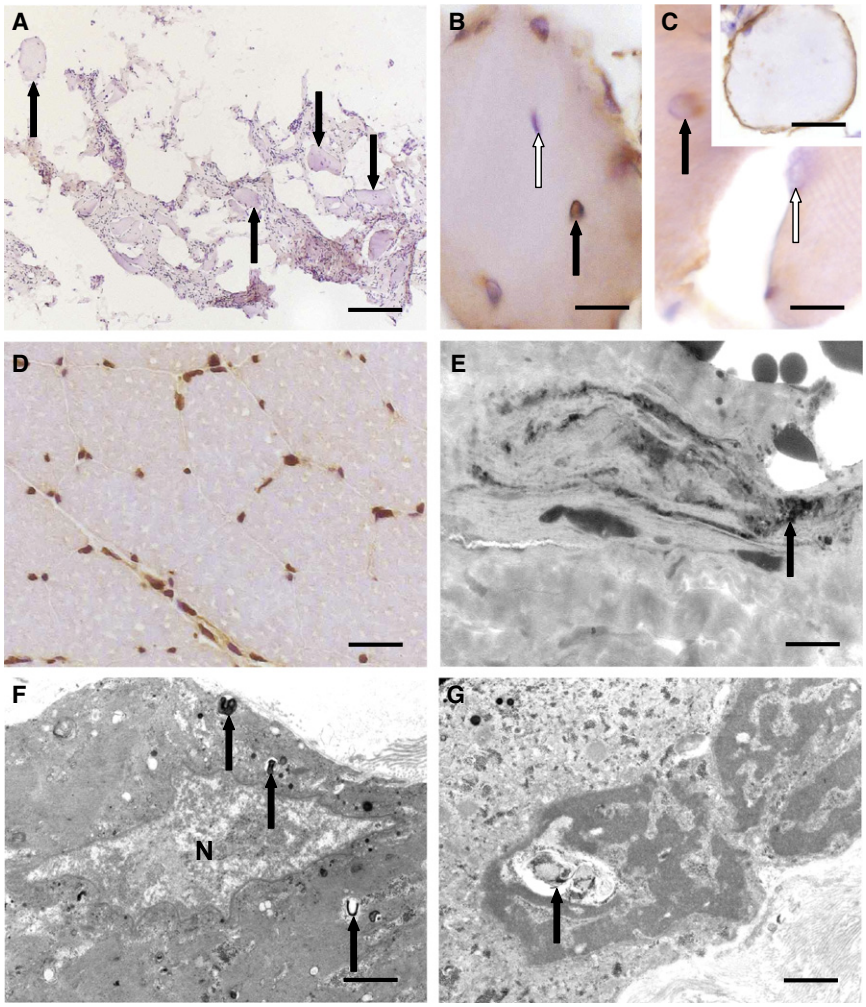

Figure 4. Muscle Biopsy Findings in VCPDM

The muscle biopsy specimen was taken from the left M. gastrocnemius of a 54-year-old male patient of the Bulgarian family.

(A) The muscle parenchyma is largely replaced by fat and connective tissue. The remaining muscle fibers show a high degree of caliber variability. Hypertrophic muscle fibers containing nonsubsarcolemmal nuclei are marked by arrows. A hematoxylin stain was used on the cryostat section. The scale bar represents 250 μm.

(B and C) Matrin 3 immunostaining (rabbit anti-matrin 3 antibody BL2526; Bethyl Labs, Montgomery, TX, USA) of cryosectioned muscle fibers showing variable degrees of immunoreactivity of myonuclei (black arrows, immunoreactive nuclei labeled by brown reaction product; white arrows, faintly stained or almost unlabelled myonuclei). Because of the vast proliferation of fat tissue, the cryostat sections had to be cut much thicker than normal, 15 μm, resulting in a blurry appearance of the nuclei. A hematoxylin counterstain was used. The scale bar represents 40 μm in (B) and 25 μm in (C). The inset in (C) shows a muscle fiber with intact sarcolemmal dystrophin immunoreactivity (Dys 1 antibody, Novocastra, Newcastle, UK) indicating preserved overall immunoreactivity of the biopsied tissue. The scale bar represents 50 μm.

(D) Normal control muscle immunostained with the matrin 3 antibody: Strong immunoreactivity of all myonuclei. A hematoxylin counterstain was used on the cryostat section. The scale bar represents 50 μm.

(E) Semithin section of biopsy tissue that was cut from the block of frozen tissue, thawed, fixed in 6% buffered glutaraldehyde, and embedded in epoxy resin. Two muscle fibers are surrounded by fibrotic connective tissue and fat cells. Dark, osmiophilic material has accumulated in both fibers. The arrow indicates a strongly osmiophilic deposit, most likely autophagic material. A paraphenylene diamine stain was used. The scale bar represents 20 μm.

(F and G) Electron microscopy of ultrathin sections of the resin-embedded tissue. In (F), this muscle fiber shows an irregularly shaped nucleus with loose chromatin and numerous small perinuclear autophagic vacuoles containing osmiophilic, often myelin-like material. The scale bar represents 3 μm. In (G), two irregular, preapoptotic myonuclei are shown. One of the nuclei embraces an autophagic vacuole (indicated by an arrow), probably as a result of sarcoplasmic invagination. The scale bar represents 2 μm.

Heisenberg fellow and C. Stendel is a postdoctoral fellow of the Deutsche Forschungsgemeinschaft. A. Roos received a PhD scholarship from Aachen University of Technology. This work was supported by grants from the START program of the Faculty of Medicine of Aachen University of Technology (to M. Elbracht), the Doktor Robert Pfleger-Stiftung and the Maximilian May-Stiftung (to J. Senderek), the Swiss National Science Foundation (to J.S.B.), the Bulgarian Ministry of Education and Science (to V.G., V.M., and I.T.), and the Interdisciplinary Centre for Clinical Research BIOMAT within the Faculty of Medicine of Aachen University of Technology (to J.S. and J.W.).

Received: January 5, 2009
Revised: February 19, 2009
Accepted: March 10, 2009
Published online: April 2, 2009

Web Resources

The URLs for data presented herein are as follows:

European Bioinformatics Institute Web site (for ClustalW), http://www.ebi.ac.uk/index.html

GeneCards Human Gene Database (for data on positional candidate genes), http://www.genecards.org

HUGE protein database (for matrin 3 [KIAA0723]), http://www.kazusa.or.jp/huge/index.html

Human genome assembly (for chromosome 5q31), http://genome.ucsc.edu

National Center for Biotechnology Information (NCBI; for data on positional candidate genes and matrin 3 orthologs (RefSeq, Pubmed, OMIM, Gene, Protein), http://www.ncbi.nlm.nih.gov

NCBI blast server (for protein sequence alignments), http://blast.ncbi.nlm.nih.gov/Blast.cgi

NCBI dbSNP repository (for single-nucleotide polymorphisms), http://www.ncbi.nlm.nih.gov/SNP

PolyPhen algorithm (for prediction of the S85C mutation effect), http://genetics.bwh.harvard.edu/pph/

SIFT algorithm (for prediction of the S85C mutation effect), http://blocks.fhcrc.org/sift/SIFT.html

SMART program (for the analysis of protein domain structure and composition), http://smart.embl-heidelberg.de

subPSEC algorithm (for prediction of the S85C mutation effect), http://www.pantherdb.org/tools/csnpScoreForm.jsp

References

1. Udd, B., and Griggs, R. (2001). Distal myopathies. Curr. Opin. Neurol. *14*, 561–566.
2. Udd, B. (2007). Molecular biology of distal muscular dystrophies-sarcomeric proteins on top. Biochim. Biophys. Acta *1772*, 145–158.
3. Bashir, R., Britton, S., Strachan, T., Keers, S., Vafiadaki, E., Lako, M., Richard, I., Marchand, S., Bourg, N., Argov, Z., et al. (1998). A gene related to Caenorhabditis elegans spermatogenesis factor fer-1 is mutated in limb-girdle muscular dystrophy type 2B. Nat. Genet. *20*, 37–42.
4. Liu, J., Aoki, M., Illa, I., Wu, C., Fardeau, M., Angelini, C., Serrano, C., Urtizberea, J.A., Hentati, F., Hamida, M.B., et al. (1998). Dysferlin, a novel skeletal muscle gene, is mutated in Miyoshi myopathy and limb girdle muscular dystrophy. Nat. Genet. *20*, 31–36.
5. Tateyama, M., Aoki, M., Nishino, I., Hayashi, Y.K., Sekiguchi, S., Shiga, Y., Takahashi, T., Onodera, Y., Haginoya, K., Kobayashi, K., et al. (2002). Mutation in the caveolin-3 gene causes a peculiar form of distal myopathy. Neurology *58*, 323–325.
6. Hackman, P., Vihola, A., Haravuori, H., Marchand, S., Sarparanta, J., De Seze, J., Labeit, S., Witt, C., Peltonen, L., Richard, I., et al. (2002). Tibial muscular dystrophy is a titinopathy caused by mutations in TTN, the gene encoding the giant skeletal-muscle protein titin. Am. J. Hum. Genet. *71*, 492–500.
7. Meredith, C., Herrmann, R., Parry, C., Liyanage, K., Dye, D.E., Durling, H.J., Duff, R.M., Beckman, K., de Visser, M., van der Graaff, M.M., et al. (2004). Mutations in the slow skeletal muscle fiber myosin heavy chain gene (MYH7) cause laing early-onset distal myopathy (MPD1). Am. J. Hum. Genet. *75*, 703–708.
8. Eisenberg, I., Avidan, N., Potikha, T., Hochner, H., Chen, M., Olender, T., Barash, M., Shemesh, M., Sadeh, M., Grabov-Nardini, G., et al. (2001). The UDP-N-acetylglucosamine 2-epimerase/N-acetylmannosamine kinase gene is mutated in recessive hereditary inclusion body myopathy. Nat. Genet. *29*, 83–87.
9. Feit, H., Silbergleit, A., Schneider, L.B., Gutierrez, J.A., Fitoussi, R.P., Réyès, C., Rouleau, G.A., Brais, B., Jackson, C.E., Beckmann, J.S., et al. (1998). Vocal cord and pharyngeal weakness with autosomal dominant distal myopathy: Clinical description and gene localization to 5q31. Am. J. Hum. Genet. *63*, 1732–1742.
10. Salmikangas, P., van der Ven, P.F., Lalowski, M., Taivainen, A., Zhao, F., Suila, H., Schröder, R., Lappalainen, P., Fürst, D.O., and Carpén, O. (2003). Myotilin, the limb-girdle muscular dystrophy 1A (LGMD1A) protein, cross-links actin filaments and controls sarcomere assembly. Hum. Mol. Genet. *12*, 189–203.
11. Hauser, M.A., Horrigan, S.K., Salmikangas, P., Torian, U.M., Viles, K.D., Dancel, R., Tim, R.W., Taivainen, A., Bartoloni, L., Gilchrist, J.M., et al. (2000). Myotilin is mutated in limb girdle muscular dystrophy 1A. Hum. Mol. Genet. *9*, 2141–2147.
12. Selcen, D., and Engel, A.G. (2004). Mutations in myotilin cause myofibrillar myopathy. Neurology *62*, 1363–1371.
13. Foroud, T., Pankratz, N., Batchman, A.P., Pauciulo, M.W., Vidal, R., Miravalle, L., Goebel, H.H., Cushman, L.J., Azzarelli, B., Horak, H., et al. (2005). A mutation in myotilin causes spheroid body myopathy. Neurology *65*, 1936–1940.
14. Garvey, S.M., Senderek, J., Beckmann, J.S., Seboun, E., Jackson, C.E., and Hauser, M.A. (2006). Myotilin is not the causative gene for vocal cord and pharyngeal weakness with distal myopathy (VCPDM). Ann. Hum. Genet. *70*, 414–416.
15. Belgrader, P., Dey, R., and Berezney, R. (1991). Molecular cloning of matrin 3. A 125-kilodalton protein of the nuclear matrix contains an extensive acidic domain. J. Biol. Chem. *266*, 9893–9899.
16. Hibino, Y., Usui, T., Morita, Y., Hirose, N., Okazaki, M., Sugano, N., and Hiraga, K. (2006). Molecular properties and intracellular localization of rat liver nuclear scaffold protein P130. Biochim. Biophys. Acta *1759*, 195–207.
17. Berezney, R., Mortillaro, M.J., Ma, H., Wei, X., and Samarabandu, J. (1995). The nuclear matrix: A structural milieu for genomic function. Int. Rev. Cytol. *162A*, 1–65.
18. Pederson, T. (2000). Half a century of "the nuclear matrix". Mol. Biol. Cell *11*, 799–805.
19. Berezney, R., and Wei, X. (1998). The new paradigm: Integrating genomic function and nuclear architecture. J. Cell. Biochem. Suppl. *30–31*, 238–242.
20. Munkel, C., Eils, R., Dietzel, S., Zink, D., Mehring, C., Wedemann, G., Cremer, T., and Langowski, J. (1999). Compartmentalization of interphase chromosomes observed in simulation and experiment. J. Mol. Biol. *285*, 1053–1065.
21. Boulikas, T. (1995). Chromatin domains and prediction of MAR sequences. Int. Rev. Cytol. *162A*, 279–388.
22. Heng, H.H., Goetze, S., Ye, C.J., Liu, G., Stevens, J.B., Bremer, S.W., Wykes, S.M., Bode, J., and Krawetz, S.A. (2004). Chromatin loops are selectively anchored using scaffold/matrix-attachment regions. J. Cell Sci. *117*, 999–1008.
23. Goetze, S., Mateos-Langerak, J., and van Driel, R. (2007). Three-dimensional genome organization in interphase and its relation to genome function. Semin. Cell Dev. Biol. *18*, 707–714.
24. Hutchison, C.J., Bridger, J.M., Cox, L.S., and Kill, I.R. (1994). Weaving a pattern from disparate threads: Lamin function in nuclear assembly and DNA replication. J. Cell Sci. *107*, 3259–3269.
25. Lattanzi, G., Cenni, V., Marmiroli, S., Capanni, C., Mattioli, E., Merlini, L., Squarzoni, S., and Maraldi, N.M. (2003). Association of emerin with nuclear and cytoplasmic actin is regulated in differentiating myoblasts. Biochem. Biophys. Res. Commun. *303*, 764–770.
26. Nickerson, J.A., Krockmalnic, G., Wan, K.M., and Penman, S. (1997). The nuclear matrix revealed by eluting chromatin from a cross-linked nucleus. Proc. Natl. Acad. Sci. USA *94*, 4446–4450.
27. Parnaik, V.K., and Manju, K. (2006). Laminopathies: Multiple disorders arising from defects in nuclear architecture. J. Biosci. *31*, 405–421.
28. Bione, S., Maestrini, E., Rivella, S., Mancini, M., Regis, S., Romeo, G., and Toniolo, D. (1994). Identification of a novel X-linked gene responsible for Emery-Dreifuss muscular dystrophy. Nat. Genet. *8*, 323–327.

29. Bonne, G., Di Barletta, M.R., Varnous, S., Bécane, H.M., Hammouda, E.H., Merlini, L., Muntoni, F., Greenberg, C.R., Gary, F., Urtizberea, J.A., et al. (1999). Mutations in the gene encoding lamin A/C cause autosomal dominant Emery-Dreifuss muscular dystrophy. Nat. Genet. *21*, 285–288.
30. Muchir, A., Bonne, G., van der Kooi, A.J., van Meegen, M., Baas, F., Bolhuis, P.A., de Visser, M., and Schwartz, K. (2000). Identification of mutations in the gene encoding lamins A/C in autosomal dominant limb girdle muscular dystrophy with atrioventricular conduction disturbances (LGMD1B). Hum. Mol. Genet. *9*, 1453–1459.
31. De Sandre-Giovannoli, A., Chaouch, M., Kozlov, S., Vallat, J.M., Tazir, M., Kassouri, N., Szepetowski, P., Hammadouche, T., Vandenberghe, A., Stewart, C.L., et al. (2002). Homozygous defects in LMNA, encoding lamin A/C nuclear-envelope proteins, cause autosomal recessive axonal neuropathy in human (Charcot-Marie-Tooth disorder type 2) and mouse. Am. J. Hum. Genet. *70*, 726–736.
32. Wijmenga, C., Hewitt, J.E., Sandkuijl, L.A., Clark, L.N., Wright, T.J., Dauwerse, H.G., Gruter, A.M., Hofker, M.H., Moerer, P., Williamson, R., et al. (1992). Chromosome 4q DNA rearrangements associated with facioscapulohumeral muscular dystrophy. Nat. Genet. *2*, 26–30.
33. Petrov, A., Allinne, J., Pirozhkova, I., Laoudj, D., Lipinski, M., and Vassetzky, Y.S. (2008). A nuclear matrix attachment site in the 4q35 locus has an enhancer-blocking activity in vivo: Implications for the facio-scapulo-humeral dystrophy. Genome Res. *18*, 39–45.
34. Quinzii, C.M., Vu, T.H., Min, K.C., Tanji, K., Barral, S., Grewal, R.P., Kattah, A., Camaño, P., Otaegui, D., Kunimatsu, T., et al. (2008). X-linked dominant scapuloperoneal myopathy is due to a mutation in the gene encoding four-and-a-half-LIM protein 1. Am. J. Hum. Genet. *82*, 208–213.
35. Schessl, J., Zou, Y., McGrath, M.J., Cowling, B.S., Maiti, B., Chin, S.S., Sewry, C., Battini, R., Hu, Y., Cottle, D.L., et al. (2008). Proteomic identification of FHL1 as the protein mutated in human reducing body myopathy. J. Clin. Invest. *118*, 904–912.
36. Windpassinger, C., Schoser, B., Straub, V., Hochmeister, S., Noor, A., Lohberger, B., Farra, N., Petek, E., Schwarzbraun, T., Ofner, L., et al. (2008). An X-linked myopathy with postural muscle atrophy and generalized hypertrophy, termed XMPMA, is caused by mutations in FHL1. Am. J. Hum. Genet. *82*, 88–99.
37. Ng, E.K., Chan, K.K., Wong, C.H., Tsui, S.K., Ngai, S.M., Lee, S.M., Kotaka, M., Lee, C.Y., Waye, M.M., and Fung, K.P. (2002). Interaction of the heart-specific LIM domain protein, FHL2, with DNA-binding nuclear protein, hNP220. J. Cell. Biochem. *84*, 556–566.
38. Dye, B.T., and Patton, J.G. (2001). An RNA recognition motif (RRM) is required for the localization of PTB-associated splicing factor (PSF) to subnuclear speckles. Exp. Cell Res. *263*, 131–144.
39. Grantham, R. (1974). Amino acid difference formula to help explain protein evolution. Science *185*, 862–864.
40. Li, W.H., Wu, C.I., and Luo, C.C. (1984). Nonrandomness of point mutations as reflected in nucleotide substitutions in pseudogenes and its evolutionary implications. J. Mol. Evol. *21*, 58–71.
41. Miller, M.P., and Kumar, S. (2001). Understanding human disease mutations through the use of interspecific genetic variation. Hum. Mol. Genet. *10*, 2319–2328.
42. Ng, P.C., and Henikoff, S. (2001). Predicting deleterious amino acid substitutions. Genome Res. *11*, 863–874.
43. Ramensky, V., Bork, P., and Sunyaev, S. (2002). Human non-synonymous SNPs: Server and survey. Nucleic Acids Res. *30*, 3894–3900.
44. Thomas, P.D., Campbell, M.J., Kejariwal, A., Mi, H., Karlak, B., Daverman, R., Diemer, K., Muruganujan, A., and Narechania, A. (2003). PANTHER: A library of protein families and subfamilies indexed by function. Genome Res. *13*, 2129–2141.
45. Thomas, P.D., and Kejariwal, A. (2004). Coding single-nucleotide polymorphisms associated with complex vs. Mendelian disease: Evolutionary evidence for differences in molecular effects. Proc. Natl. Acad. Sci. USA *101*, 15398–15403.
46. Xi, T., Jones, I.M., and Mohrenweiser, H.W. (2004). Many amino acid substitution variants identified in DNA repair genes during human population screenings are predicted to impact protein function. Genomics *83*, 970–979.
47. Brunham, L.R., Singaraja, R.R., Pape, T.D., Kejariwal, A., Thomas, P.D., and Hayden, M.R. (2005). Accurate prediction of the functional significance of single nucleotide polymorphisms and mutations in the ABCA1 gene. PLoS Genet. *1*, e83.
48. Hibino, Y., Ohzeki, H., Sugano, N., and Hiraga, K. (2000). Transcription modulation by a rat nuclear scaffold protein, P130, and a rat highly repetitive DNA component or various types of animal and plant matrix or scaffold attachment regions. Biochem. Biophys. Res. Commun. *279*, 282–287.
49. Zhang, Z., and Carmichael, G.G. (2001). The fate of dsRNA in the nucleus: A p54(nrb)-containing complex mediates the nuclear retention of promiscuously A-to-I edited RNAs. Cell *106*, 465–475.
50. Leonard, D., Ajuh, P., Lamond, A.I., and Legerski, R.J. (2003). hLodestar/HuF2 interacts with CDC5L and is involved in pre-mRNA splicing. Biochem. Biophys. Res. Commun. *308*, 793–801.
51. Rual, J.F., Venkatesan, K., Hao, T., Hirozane-Kishikawa, T., Dricot, A., Li, N., Berriz, G.F., Gibbons, F.D., Dreze, M., and Ayivi-Guedehoussou, N. (2005). Towards a proteome-scale map of the human protein–protein interaction network. Nature *437*, 1173–1178.
52. Xu, T.R., and Rumsby, M.G. (2004). Phorbol ester-induced translocation of PKC epsilon to the nucleus in fibroblasts: Identification of nuclear PKC epsilon-associating proteins. FEBS Lett. *570*, 20–24.